JOURNAL OF CATALYSIS 57, 41–63 (1979)

# Ultradispersed Rhodium Rafts: Their Existence and Topology

D. J. C. YATES, L. L. MURRELL, AND E. B. PRESTRIDGE

*Exxon Research and Engineering Co., Linden, New Jersey 07036*

Received April 28, 1978; accepted October 16, 1978

Detailed studies have been performed on rhodium supported on alumina. Three techniques have been used in concert: chemisorption (using hydrogen and carbon monoxide), infrared spectroscopy (using adsorbed carbon monoxide), and ultra-high resolution electron microscopy. The first two techniques indicated that, under suitable reducing conditions, rhodium on alumina can not only be obtained easily in the atomically dispersed state, but that degrees of dispersion within the atomically dispersed state can be recognized and differentiated. These indications have been confirmed by electron microscopy and the existence of rafts of rhodium atoms of varying size has been shown directly. These rafts must be only one atom thick, as shown by a combination of chemisorption and microscopy on the same samples. Evidently, as we have shown that varying sizes of two-dimensional rafts occur, one can now define degrees of ultra-high dispersion. Such systems are, at the minimum, always atomically dispersed but there can be a variation in the average number of atoms in the rafts from one preparation to another. The ultimate state of ultra-high dispersion would be to have every metal atom separated from every other metal atom on the support. The smallest average raft size that we have been able to achieve so far is 1.5 nm, corresponding to each raft having an average of 8 Rh atoms. Under these conditions only two-dimensional rafts, one atom thick, could be detected; no three-dimensional cubic or spherical particles were seen on the photomicrographs. This is the best example we have been able to obtain, so far, of supported metals in the ultradispersed state.

## INTRODUCTION

The reality of atomic dispersion for certain supported metals has become more convincing with the passage of time; nevertheless many aspects of metals in this highly dispersed state are still obscure, despite intensive work in this field since 1960.

The first positive indications that atomic dispersion (in the sense that all metal atoms are in the surface) could be achieved and measured are to be found in a series of papers on supported platinum (*1–3*), using hydrogen chemisorption as the diagnostic tool. The application of hydrogen chemisorption as a sufficiently selective chemisorption process to be useful to measure accurately the dispersion of small metal particles received further impetus by a detailed study by Adams *et al.* (*4*) in 1962. They studied the dispersion of platinum on silica by three independent methods—hydrogen chemisorption, electron microscopy, and X-ray diffraction line broadening. A definitive comparison between hydrogen chemisorption data and particle sizes measured directly by electron microscopy for platinum on alumina has been published more recently by Wilson and Hall (*5*). It would appear that for those metals which dissociatively chemisorb hydrogen, one can rely on hydrogen adsorption as a good measure of average metal dispersion for supported metals.



0021-9517/79/040041-23$02.00/0

However, studies of metals in the atomically dispersed state and definitive information on the crystalline morphology of such atomically dispersed systems are almost entirely lacking, although there have been numerous theoretical studies on idealized systems (*6*, *7*). The only way in which unambiguous geometrical information can be obtained on matter in the atomically dispersed state is by ultra-high resolution electron microscopy. Such studies were first published by Prestridge and Yates (*8*) who obtained photomicrographs of rhodium atoms on silica. When aggregates were found, they were in the form of two-dimensional rafts, one atom thick. The rhodium in the same catalysts had been shown earlier to be atomically dispersed (i.e., all Rh atoms in the surface) by the hydrogen and carbon monoxide adsorption studies of Yates and Sinfelt (*9*).

Further information on well-dispersed rhodium has now been obtained. The system has been investigated by three techniques (chemisorption, infrared spectroscopy, and electron microscopy) and further evidence has been accumulated to show the correctness of the two-dimensional raft model suggested earlier. In addition, we have shown that we can differentiate between various degrees of atomic dispersion. That is, a system which has a smaller raft size is in a very real sense more highly dispersed (i.e., lower mean metal–metal coordination) than another atomically dispersed system which has a larger raft size. Both the above systems are atomically dispersed in the sense that all the metal atoms present can chemisorb a molecule from the gas phase. We propose to classify those systems containing only small rafts as ultradispersed. Such an ultradispersed system is defined as one that has a higher degree of dispersion than the minimum needed to achieve atomic dispersion.

The limiting state of ultradispersion would be a configuration where there are no rafts, pairs, etc. and each metal atom would be separated from every other metal atom on the support. The creation of such a system has not yet been achieved, as far as we are aware. The smallest average raft size we have been able to make is 1.5 nm, in other words each raft would contain on the average eight rhodium atoms.

## EXPERIMENTAL

### *Apparatus and Procedure*

*Materials and sample preparation.* The support used for this work was aluminum oxide C (surface area 100 $m^2/g$) obtained from Degussa, Inc., Teterboro, N. J. The main impurities are less than 0.2% $Fe_2O_3$ and less than 0.1% of $TiO_2$ and $SiO_2$.

To a beaker containing 125 $cm^3$ of water, 20 g of Degussa alumina was added with stirring. To this was added 75 ml of a solution containing 0.475 g of the $RhCl_3 \times H_2O$ (containing 42.09% Rh by weight). After stirring for 1 hr, the mixture was filtered. It was noted that the filtrate was colorless. The catalyst was then dried in air overnight at 120°C. The 5 and 10% Rh catalysts were prepared by incipient wetness, e.g., the 10% Rh sample was prepared by adding 7.2 ml of solution, containing 2.37 g of rhodium chloride, to 9 g of alumina. Proportional weights were used for the 5% preparation. The 5 and 10% Rh catalysts were also dried at 120°C in air after impregnation.

A small amount of work was carried out with 10% Rh supported on silica (Cabosil) prepared as described earlier (*9*).

*Infrared spectroscopy.* A detailed description of the apparatus has been given elsewhere (*10*). A Beckman grating spectrometer, Model IR7, was used which was equipped with two external mirror systems which provide accessible focused images of the Nernst source. The cell was placed at one of these foci and wire gauzes were put in the other to balance the energy in the two beams. Wider slits than usual were

used to compensate for these energy losses. The transmission of the cell with the sample in place (after reduction) varied from 25 to 44% at 2100 $cm^{-1}$. In all cases, a slit width of 0.9 mm was used at 2100 $cm^{-1}$, and the gain was varied to compensate for changes in transmission. The resolution with this slit width is shown in Table 1.

TABLE 1

Slit Widths and Resolution as a Function of Frequency in Wavenumbers

| Frequency ($cm^{-1}$) | Slit width (mm) | Resolution ($cm^{-1}$) |
|---|---|---|
| 2250 | 0.64 | 2.3 |
| 2200 | 0.73 | 2.6 |
| 2150 | 0.81 | 2.7 |
| 2100 | 0.90 | 2.8 |
| 2050 | 1.03 | 3.1 |
| 2000 | 1.08 | 3.0 |
| 1950 | 0.51 | 2.1 |
| 1900 | 0.50 | 2.0 |
| 1850 | 0.53 | 2.1 |
| 1800 | 0.56 | 2.0 |

Self-supporting discs were prepared by pressing samples in a die at about 6000 lb/in.$^2$. Sample thicknesses varied from 14 to 19 mg/cm$^2$, but were not measured in all cases. Where measured, they are given in the results section. Pieces of the disc about 2 × 0.7 cm in size were cut and and inserted in the cell. The cell was rotated so that the sample was at the silica end of the cell. Purified hydrogen, at a flow rate of 100 ml/min for a flake weighing 15 mg, was then passed through the cell. The flow rate was held at this rate of 6.7 liters/min/g for all samples. For a 200°C reduction, the sample temperature was increased at a rate of 2°C/min, while for a 450 and 480°C reduction the rate of rise was 5°C/min. The evacuation was done at about 10 to 20°C lower than the reduction temperature.

After running the background spectrum, a series of doses of carbon monoxide was added. The pressures after each addition are given in the legends to the spectra. Desorption studies at room temperature were done by direct evacuation via the diffusion pump. For elevated temperature desorption studies, the procedure is given in detail in the results section.

*Chemisorption.* The apparatus used for adsorption measurements was a conventional glass vacuum system described elsewhere (*9, 11*). Adsorption isotherms were measured by admitting a known quantity of gas to the adsorption cell and waiting for a period of about 1 hr before reading the equilibrium pressure. The apparatus was made more accurate than usual by the use of a high precision, fused quartz Bourdon pressure gauge (*12*) manufactured by the Texas Instruments Company, Houston, Tex. The high precision of this instrument is essential in accurately determining the small uptakes of gas on the low rhodium concentration samples. The smallest measurable pressure change was 0.004 cm with the particular capsule we used.

To ensure reproducible reduction conditions we standardized both the rate of rise of temperature, the reduction temperature itself, and the hydrogen flow rate per gram of sample. For example, the low temperature reductions were carried out with a hydrogen flow of 6.7 liters/min/g of catalyst. Typical catalyst charges ranged from 0.2 to 0.5 g. The temperature was linearly increased, at 2.0°C/min, to 200°C, by the use of a programmer controller model 5500/624A, obtained from Research, Inc., Minneapolis, Minn. After holding for 1 hr at 200°C, the sample was evacuated at 190°C for 10 min and then cooled to room temperature for the isotherm determination. The hydrogen flow rate is probably higher than needed, but we wished to do the reduction under identical conditions to those used in the infrared experiments. There the samples might weigh as little as 15 mg, and the lowest flow rate we felt was reasonable in the infrared unit was 100 cm$^3$/min.

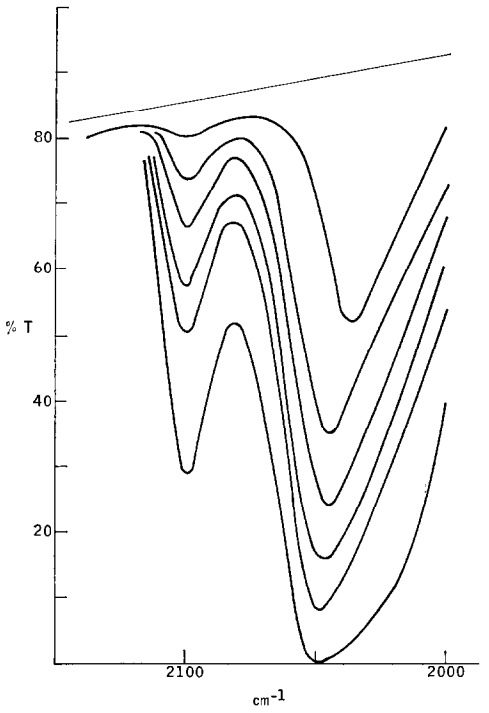


FIG. 1. Sample of 10% Rh on alumina reduced at 200°C. A series of doses of CO were added at 25°C. At full coverage both the 2100 and the 2050 $cm^{-1}$ bands had zero transmission.

For the reductions at 450°C, the flow was kept the same but the rate of rise of temperature, again linear, was 5°C/min. The hold at 450°C was for 1 hr. Evacuation was done at 430°C for 10 min.

In cases where rereduction of the same sample was done, this was performed with a lower hydrogen flow (about 250 ml/min/g) at the same rate of rise, but at 190 and 440°C, depending on the initial reduction temperature.

Before reduction, the powdered samples were pressed in a chromium plated die at 10,000 lb/in.$^2$ and then crushed to pass through a 20-mesh standard sieve, yet be retained on a 40-mesh sieve. This assured adequate gas access to the catalyst, while overcoming any problems due to fluidization of the catalyst bed during reduction.

*Electron microscopy.* The sample preparations and experimental techniques were similar to those used in the earlier work on rhodium supported on silica (*8*).

A Philips EM-300 microscope was used with high resolution pole pieces. To maximize the difference in the elastic scattering of electrons by light and heavy atoms, we employed a 30-$\mu$m objective aperture as discussed in detail earlier (*8*).

The catalyst samples in all cases were taken from the identical sample flake used in the infrared studies at the end of the experiments, hence the rhodium was in the reduced state. The flake was ground and ultrasonically dispersed in butyl alcohol and deposited on a "holey" carbon film. Electron micrographs were printed (final magnification: 1,000,000×) using a point-source enlarger. The magnification was calibrated using the $\gamma$-alumina lattice as an internal standard and is considered accurate to ±2%. Figure 16 shows both the 0.790-nm unit cell and the 0.456-nm spacing of the (111) planes. Particle size distributions were determined by measurements made on the micrographs.

## RESULTS

Figure 1 shows the infrared spectra of CO adsorbed onto 10% Rh on alumina reduced at the low temperature of 200°C. It will be seen that there are two bands—a high frequency one at 2100 $cm^{-1}$ and an asymmetric band at lower frequencies. At low coverages the latter band is at about 2030 $cm^{-1}$, moving to 2050 $cm^{-1}$ at the highest dose shown. At saturation with this particular sample, both the 2100 and 2050 $cm^{-1}$ bands were blackouts.

To obtain information over the full CO coverage range, a sample containing 1% Rh (thickness 15 mg/cm$^2$, of total weight 15 mg) was put in the cell and reduced for 1.5 hr at 200°C. From the pressures before and after adsorption, given in the legend of Fig. 2, it will be seen that the first four doses were at coverages less than a monolayer. Saturation (or monolayer) coverage

was reached with the fifth dose, with a final pressure of 0.15 cm. Many experiments have shown that no more CO is adsorbed once a pressure (after adsorption) of about 1 mm is reached. The spectrum of this sample is entirely different from the 10% Rh sample, as it is evident that two symmetrical bands dominate the spectrum at 2100 and 2025 $cm^{-1}$. Study of the high transmission region between these bands (i.e., approximately 2030–2080 $cm^{-1}$) shows a change of slope occurring with increasing dosage at about 2075 $cm^{-1}$.

This is also shown in the desorption studies of Fig. 3. The desorption procedure was as follows. After recording the spectrum after dose 5 was added, the sample was evacuated via the diffusion pump for 80 min at room temperature. After recording the spectra, the cell was reconnected to the vacuum system and then rotated to bring the sample to the silica end of the cell. The furnace was then placed around the cell and rapidly heated to 100°C. After 17 min at 100°C, the furnace was removed, the cell was rotated through 180°, and the spectra were recorded again. The identical procedure was used for all desorption experiments.

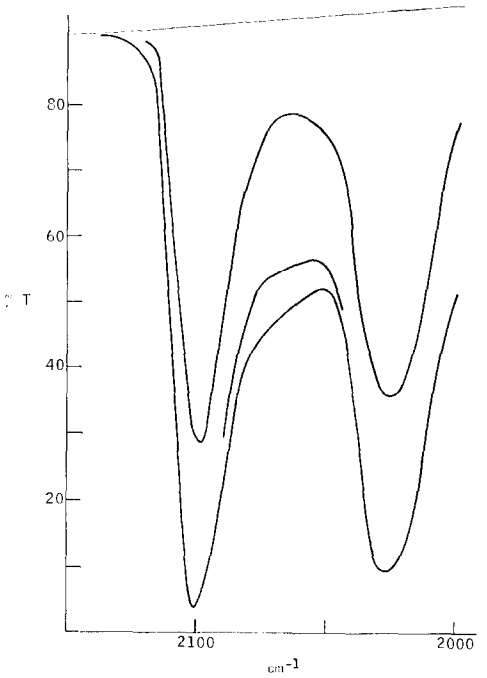


FIG. 3. Desorption of CO from the sample used in Fig. 2. Spectra shown are for: the fifth dose of CO (0.15 cm), after evacuation at 25°C for 80 min, and finally after evacuation at 100°C for 17 min. The top line is the spectra recorded before CO addition.

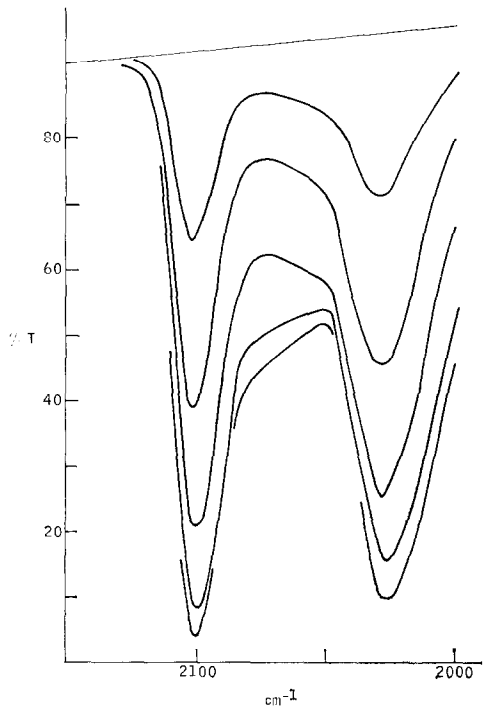


FIG. 2. Sample of 1% Rh on alumina reduced at 200°C. Transmission at 2100 $cm^{-1}$ before adding CO was 44%. The pressure of CO after the first four doses was zero. The pressure after the fifth dose was 0.15 cm.

To show the effect of reduction temperature, another sample of 1% Rh was put in the cell and reduced for 1 hr at 480°C. The sample weighed 24 mg, and had a thickness of 19 $mg/cm^2$. Spectra obtained from this sample are shown in Figs. 4 and 5. The strongest bands in Fig. 4 have about 15% transmission, while the corresponding bands in Fig. 2 had a transmission of only 3%. This relative decrease in intensity of the sample of Fig. 4 occurred despite the fact that the thickness of the sample used

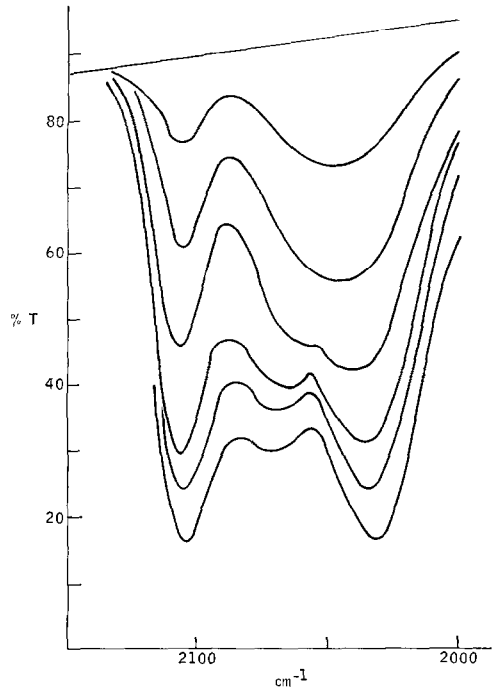


FIG. 4. Sample of 1% Rh on alumina reduced at 480°C. The pressure of CO after the first five doses was zero. The pressure after the sixth dose was 0.08 cm.

in Fig. 4 was 19 mg/cm$^2$ and that used in Fig. 2 was 15 mg/cm$^2$. The other major difference is that the band at 2075 cm$^{-1}$, which was only evident as a shoulder in the 200°C reduced sample, is now clearly resolved at high coverage in the 480°C reduced sample (see doses 4 to 6 in Fig. 4). This 2075 cm$^{-1}$ band is due to a species which is much more weakly held than that producing the bands at 2100 and 2025 cm$^{-1}$ as shown by the desorption studies of Fig. 5.

As a result of these studies with dilute rhodium systems, it now becomes possible to understand the very complex spectra of the 10% Rh systems. To bring intensities into the region where spectra could be recorded in optical density, the 10% Rh sample was diluted on an equal weight basis with Degussa alumina, giving an effective Rh concentration of 5%, although the local concentration of the Rh was still 10%. The sample had a thickness of 14 mg/cm$^2$ and was reduced at 480°C for 1 hr. Figure 6 shows that at low coverage only one strong band was seen at 2055 cm$^{-1}$, while another band at 2100 cm$^{-1}$ became evident at higher coverages. At saturation (dose 6) the 2055 cm$^{-1}$ band had moved to about 2070 cm$^{-1}$, while a band at about 2025 cm$^{-1}$ was found on the low frequency side of the 2070 cm$^{-1}$ band. For strongly held species such as CO on Rh, data obtained on adsorption are clearly, in general, in a nonequilibrium configuration. Spectra more characteristic of equilibrium are obtained by desorption. Figure 7 shows that the central band moves from 2072 cm$^{-1}$ with CO present, to 2062 cm$^{-1}$ after evacuation for 60 min at 25°C. Evacuation at 100°C for 15 min moves the band to 2045 cm$^{-1}$ and it is found at 2030 cm$^{-1}$ after a 200°C evacuation for 20 min. Only a very weak

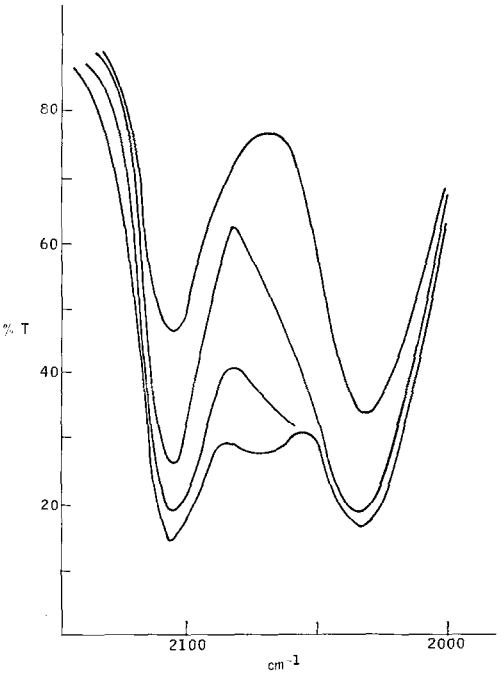


FIG. 5. Desorption of CO from the sample used in Fig. 4. Spectra shown are for: the sixth dose of CO (0.08 cm), after evacuation at 25°C for 80 min, after evacuation at 100°C for 15 min, and finally after evacuation at 200°C for 15 min.

band at 2025 $cm^{-1}$ is found after evacuation for 25 min at 250°C. Evidently there is a wide range of heterogeneity in the particular CO species producing the 2030–2072 $cm^{-1}$ bands. Another problem is that the overlap of the 2025 and 2072 $cm^{-1}$ bands makes it difficult to know if the relatively weakly held species producing the 2072 $cm^{-1}$ band has a single frequency or has varying apparent peak positions due to severe band overlap.

To show that the species of CO giving the band at about 2075 $cm^{-1}$ is associated with high temperatures of reduction rather than solely with high local Rh concentrations, experiments were done with low temperature reductions of the sample containing 10% Rh. The only way in which this could be done without causing blackouts due to the strong peaks at saturation was by diluting the 10% Rh with alumina

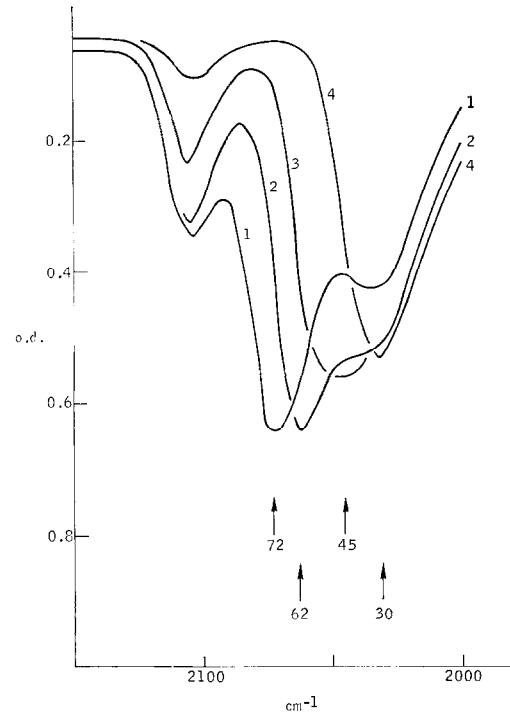


FIG. 7. Desorption of CO from the sample used in Fig. 6. Spectra: 1, dose 5 from Fig. 6; 2, after evacuation at 25°C for 60 min; 3, after evacuation at 100°C for 15 min; 4, after evacuation at 200°C for 20 min. A very weak band was present at 2025 $cm^{-1}$ after evacuation at 250°C for 25 min.

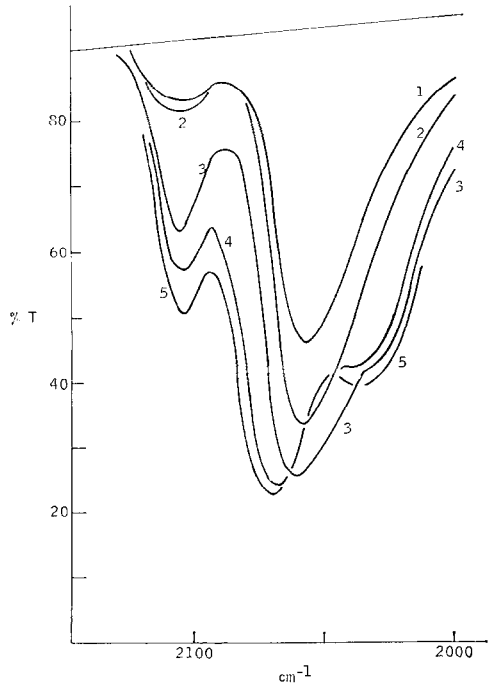


FIG. 6. Sample of 5% Rh on alumina (diluted from 10%) reduced at 480°C. The pressure of CO after the first four doses was zero. The pressure after the fifth dose was 0.14 cm.

so that the overall concentration was 2%. The data are shown in Fig. 8. At low coverage a narrow 2100 $cm^{-1}$ band and a broad band at 2045 $cm^{-1}$ are the only bands present. At higher coverages the 2045 $cm^{-1}$ band gradually splits into two bands, one at 2070 $cm^{-1}$ and the other at 2030 $cm^{-1}$. The main difference between the 10% Rh (diluted to 2%) shown in Fig. 8 and the 1% Rh shown in Fig. 2 is that the 2075 $cm^{-1}$ band is fairly intense in Fig. 8, while it is only evident as a weak shoulder in Fig. 2. In both cases, the reduction was carried out at 200°C. No quantitative value can easily be obtained of the relative number of CO molecules producing the 2075 $cm^{-1}$ bands in Fig. 8 as this band is of unknown half-width and is obviously

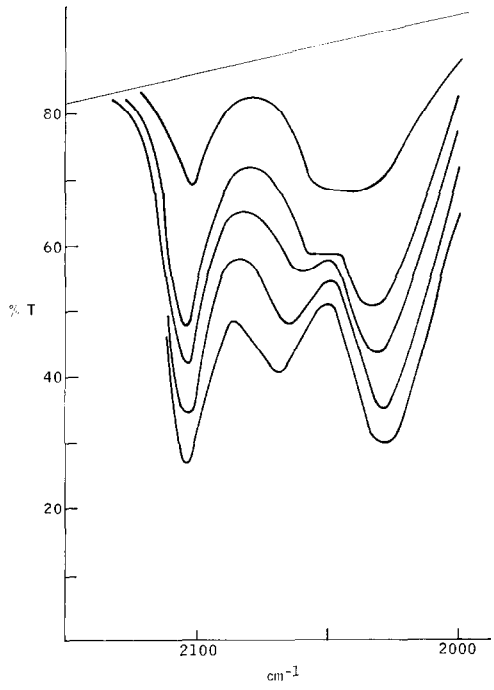


FIG. 8. Sample of 2% Rh (diluted from 10%) on alumina reduced at 200°C. The pressure of CO after the first three doses was zero. The pressure after the fourth dose was 0.16 cm and after the fifth dose 7.3 cm.

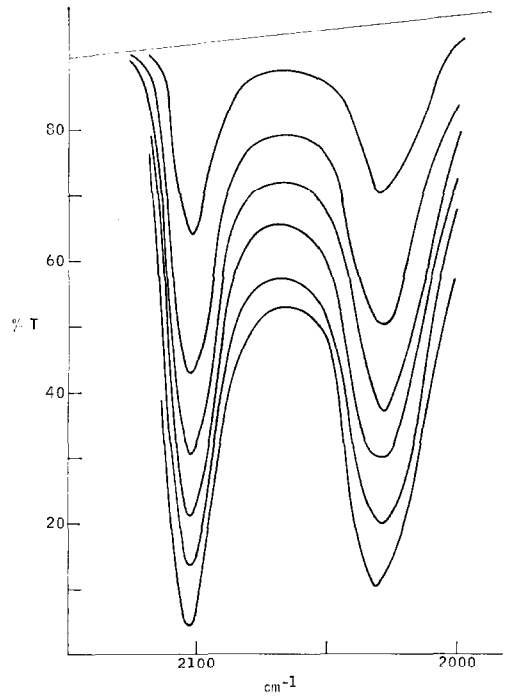


FIG. 9. Sample of 1% Rh reduced at 200°C. The pressure of CO after all six doses was zero. After dose 7, the pressure was 0.045 cm and the 2100 $cm^{-1}$ band had a transmission of 2%. After dose 8, the pressure was 0.27 cm and the 2100 $cm^{-1}$ band was a blackout.

overlapped considerably by the 2030 and 2100 $cm^{-1}$ bands.

In our early experiments we considered that samples which were highly dispersed contained few, if any, adsorbed CO molecules attached to two Rh atoms—the so-called bridged CO. To check this, we prepared a fairly thick sample containing 1% Rh and reduced it at 200°C. Figure 9 shows the linear CO region between 2000 and 2150 $cm^{-1}$ and at the highest coverage shown the 2105 $cm^{-1}$ band had a transmission of about 3%. The thickness of the sample used in Fig. 9 was not measured, but comparison with Fig. 2 shows that its thickness must be close to 15 $mg/cm^2$. It is of interest that this sample (Fig. 9) shows no evidence of a band at 2075 $cm^{-1}$. Because of this, the half-width of the 2105 $cm^{-1}$ band was only measured on this spectrum. It was 15 $cm^{-1}$, which is very narrow indeed for a band of adsorbed CO.

Figure 10 shows the bridged region (between 1800 and 2000 $cm^{-1}$) for doses 1 and 6 of the spectra shown in Fig. 9. A very weak, broad band is seen at about 1840 $cm^{-1}$. Evidently the vast majority of CO

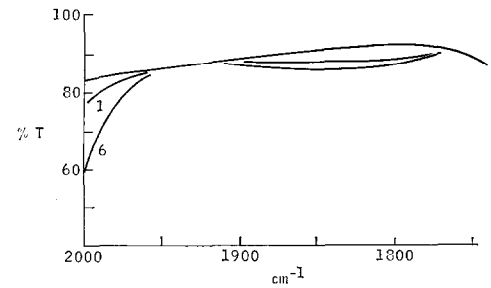


FIG. 10. The bridged region for the sample used in Fig. 9. Spectra shown of background before adding CO and doses 1 and 6.

adsorbed on the sample used to obtain Figs. 9 and 10 is in the linear form. Other observations we have made with less highly dispersed samples show the presence of stronger bridged bands. In general, for most metals and certainly for Rh, it seems that the higher the dispersion the less the intensity of the bridged band. This is reinforced by comparing the relative intensities of the linear and bridged CO bands of poorly dispersed 10% Rh on silica (*13*) (no band at 2100 $cm^{-1}$) and of Rh films evaporated in gaseous CO (*14*), or of Rh films evaporated in ultra-high vacua (*15*). As the particle size of the Rh increases, the bridged band becomes more intense relative to the linear band.

Finally an interesting effect of adsorbed CO on the mobility of Rh atoms was observed and is shown in the spectra of Fig.

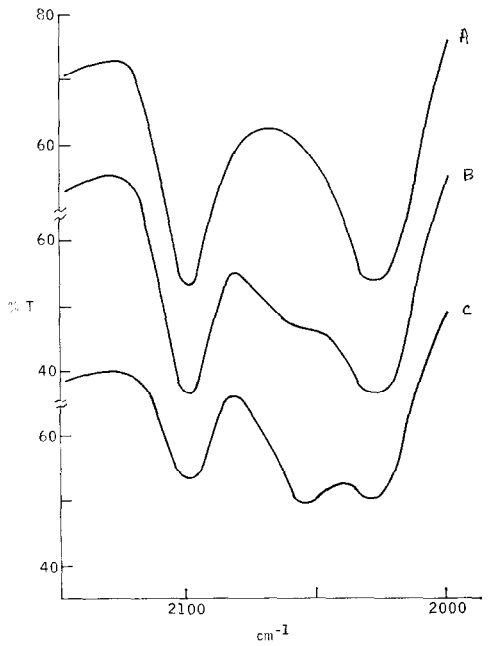


FIG. 11. The effect of rereduction on the spectra of CO adsorbed on 1% Rh on alumina. Spectra: A, after the first dose of CO added after the initial reduction at 200°C; B, after the first dose of CO added after rereduction at 180°C; C, after the first dose of CO added after a second rereduction at 180°C.

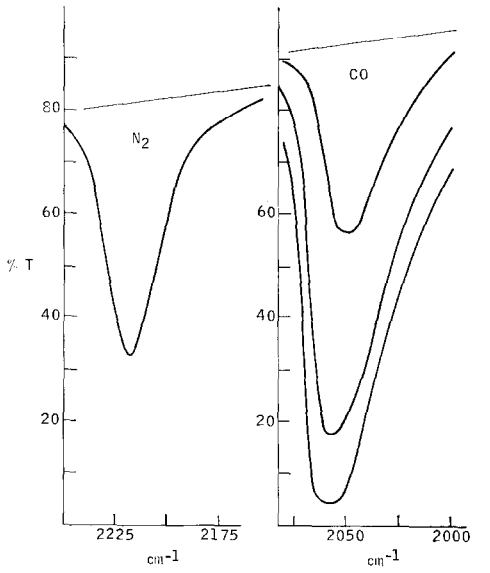


FIG. 12. Sample of 10% Rh on alumina reduced at 500°C. Spectra of $N_2$ adsorbed at a final pressure of 12 cm. The $N_2$ was evacuated for 30 sec at 25°C then CO was adsorbed. The pressure of CO after the first three doses was zero. For dose 4 the pressure was zero, but the peak at 2070 $cm^{-1}$ was a blackout.

11. A 1% Rh sample was reduced at 200°C and a series of CO doses was added to saturation. The spectra after the first of these doses (about 50% of saturation) with initial pressure of 0.08 cm is shown in Fig. 11A. Further doses of CO were added until the monolayer was saturated. After evacuation of the excess CO at room temperature for 90 min, hydrogen was passed through the cell at 200 $cm^3$/min and the sample was rereduced at 180°C with the rate of rise of temperature being identical to that used in the initial reduction (2°C/min). After rereduction at 180°C for 1 hr, the sample was evacuated at 180°C and cooled to room temperature. No adsorbed CO was present after this rereduction. After adding a dose of CO (initial pressure 0.085 cm) almost the same as that used in Fig. 11A, spectrum 11B was obtained. Now a band at about 2055 $cm^{-1}$ is present with significant intensity, in addition to the ubiquitous bands at 2100 and 2030 $cm^{-1}$. When the sample was reduced for the third

time and CO adsorbed, the spectra shown in Fig. 11C was obtained. Now the 2055 $cm^{-1}$ band is stronger than the 2030 $cm^{-1}$ band and the 2055 $cm^{-1}$ band dominates the spectrum.

Nitrogen adsorption has been studied only briefly on silica-supported rhodium (*16*), most work having been done on nickel (*17–20*), while much less work has been done with palladium (*18*), platinum (*18, 21*), and iridium (*22*). In view of this, we thought it of interest to study the adsorption of nitrogen over a range of rhodium concentrations and dispersions.

Data obtained for a 10% Rh sample reduced at 500°C for 2 hr are shown in Fig. 12A. The nitrogen band (at 25°C) did not change in shape or peak position as a function of coverage from that shown in Fig. 12A. The peak is at 2220 $cm^{-1}$. The nitrogen, as expected from all earlier work, was very weakly chemisorbed, an evacuation of 30 sec with the diffusion pump removing all the adsorbed material. To enable comparison to be made with the intensity of adsorbed CO, after evacuating the $N_2$ at 25°C, CO was adsorbed, the spectra of the first three doses being shown in Fig. 12B. For dose 4 and subsequent doses, the peak at 2070 $cm^{-1}$ was a blackout. Evidently, if the extinction coefficient for $N_2$ on Rh is similar to that of $N_2$ on Ni, then much less of the Rh surface can adsorb $N_2$ than can adsorb CO.

Note that the 10% Rh sample reduced at 500°C has no band at 2100 $cm^{-1}$. There may be a band at 2030 $cm^{-1}$, but if so, it is almost certainly hidden under the dominant 2070 $cm^{-1}$ band.

When samples were studied which had strong 2100 and 2030 $cm^{-1}$ CO bands, we were never able to detect the spectra of adsorbed $N_2$. In general, the procedure we followed was to reduce the sample, evacuate at or slightly less than the temperature of reduction, then cool to room temperature in vacuum. After running the background spectrum over the region 2000 to 2300 $cm^{-1}$,

TABLE 2

Carbon Monoxide and Hydrogen Chemisorption Data for Rhodium on Alumina

| Rhodium conc. (wt%) | Reduction | | H/M[a] | CO/M[b] | Crystallite size (nm)[c] |
|---|---|---|---|---|---|
| | Number per sample | °C | | | |
| 1 | 1st | 200 | 1.16 (5) | — | 1.1 |
| | 2nd | 180 | — | 1.73 (5) | — |
| | 3rd | 180 | — | 1.19 (2) | — |
| 1 | 1st | 465 | 1.06 (2) | — | 1.1 |
| | 2nd | 450 | — | 1.46 (2) | — |
| | 3rd | 450 | — | 1.30 (1) | — |
| 10 | 1st | 200 | 0.50 (2) | — | 2.1 |
| | 2nd | 180 | — | 0.78 (2) | — |
| | 3rd | 180 | — | 0.54 (2) | — |
| 10 | 1st | 480 | 0.54 (2) | — | 2.0 |
| | 2nd | 450 | — | 0.46 (2) | — |
| | 3rd | 450 | — | 0.36 (2) | — |

[a] Atoms of hydrogen adsorbed per Rh atom at 10 cm pressure.

[b] Molecules of carbon monoxide adsorbed per Rh atom at 10 cm pressure.

[c] Calculated from $H_2$ adsorption data with the shape of the particles assumed to be spheres or cubes.

TABLE 3

Comparison of Hydrogen and Carbon Monoxide Adsorptions on Supported Rhodium, as a Function of Metal Concentration and Reduction Temperature

| Rhodium conc. (wt%) | H/M | | | | CO/M | | | |
|---|---|---|---|---|---|---|---|---|
| | A | B | C | D | A | B | C | D |
| 10 | 0.48 | — | 0.54 (2) | 0.50 (2) | 0.44 | — | 0.46 (2) | 0.78 (2) |
| 5 | 0.59 | 0.75 | 0.51 (1) | 0.51 (1) | 0.52 | 0.75 | 0.44 (1) | 0.67 (1) |
| 1 | 0.94 | 1.0 | 1.06 (2) | 1.16 (5) | 1.01 | 1.45 | 1.46 (2) | 1.73 (5) |

Authors, supports, and reduction details

| Column | Support | Reduction temperature (°C) | Reference |
|---|---|---|---|
| A | $SiO_2$ (Cabosil) | 450 | (*9*) |
| B | $Al_2O_3$ (Davison) | 500 | (*30*) |
| C | $Al_2O_3$ (Degussa) | 470 | This work |
| D | $Al_2O_3$ (Degussa) | 200 | This work |

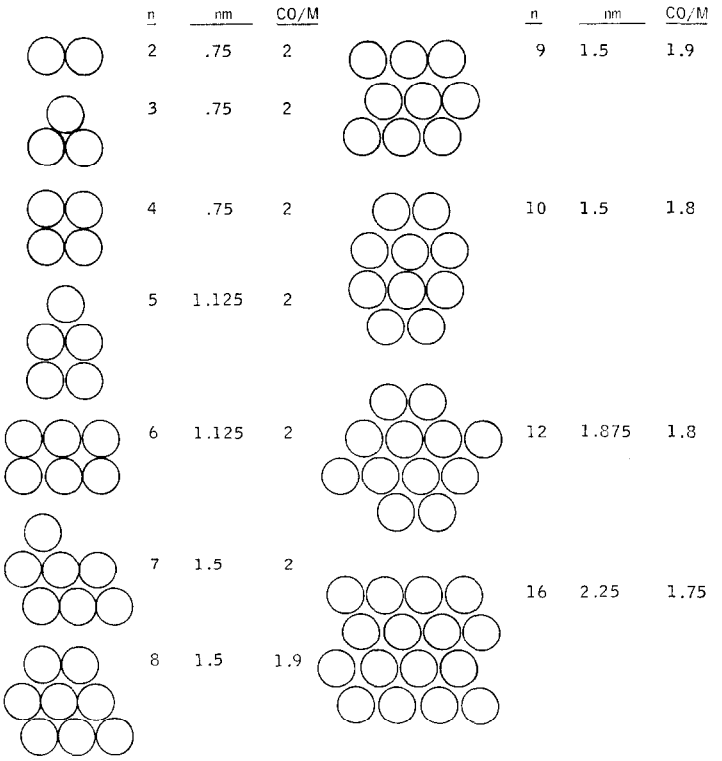


FIG. 13. Model of the packing of two-dimensional rafts of rhodium, as a function of the number of atoms ($n$), the diameter in nanometers (nm), and the CO/M ratio. Based on measured average packing spacing of Rh on $SiO_2$ of 0.375 nm (*8*).

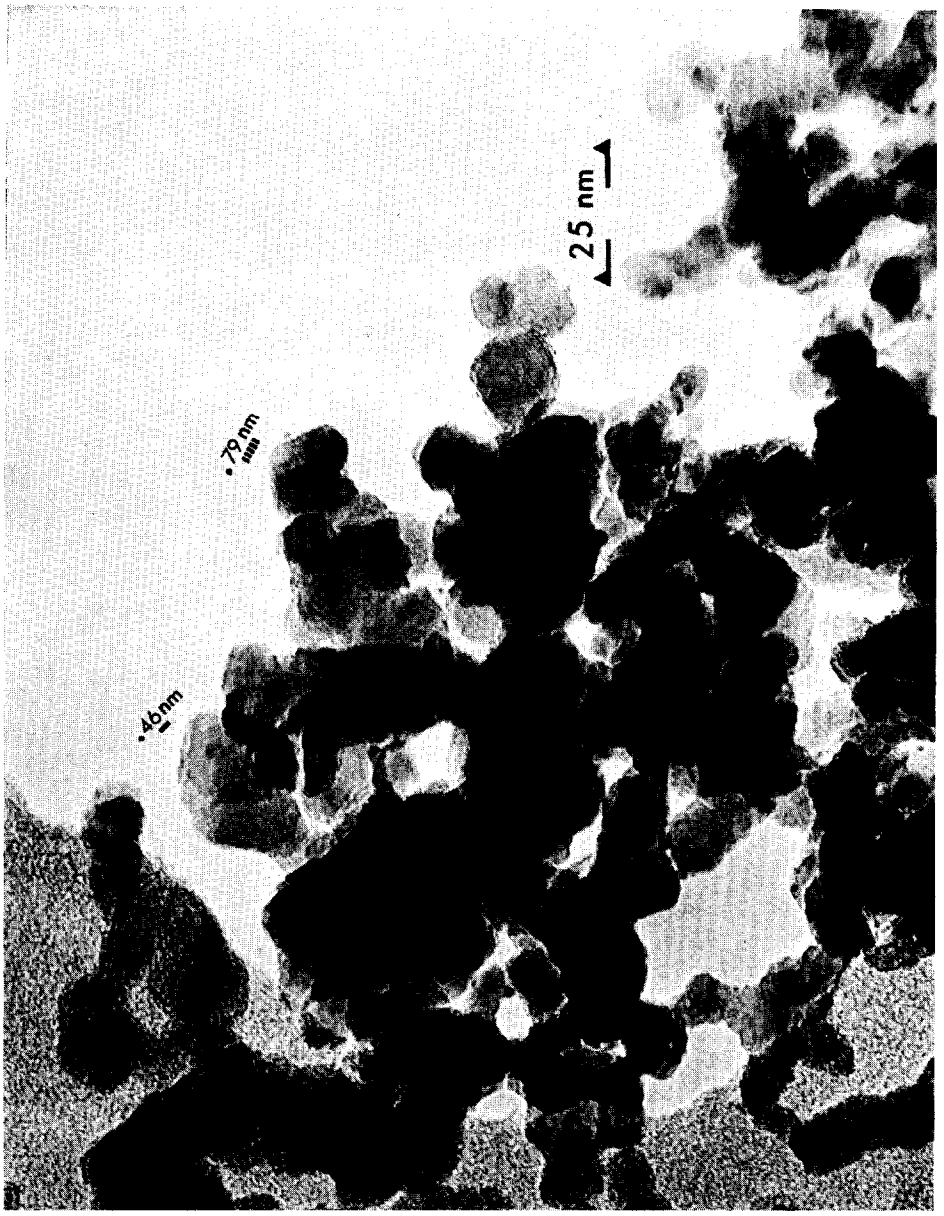


FIG. 14. Photomicrograph of the 1% Rh sample used in Fig. 2 (original magnification $1 \times 10^6$).

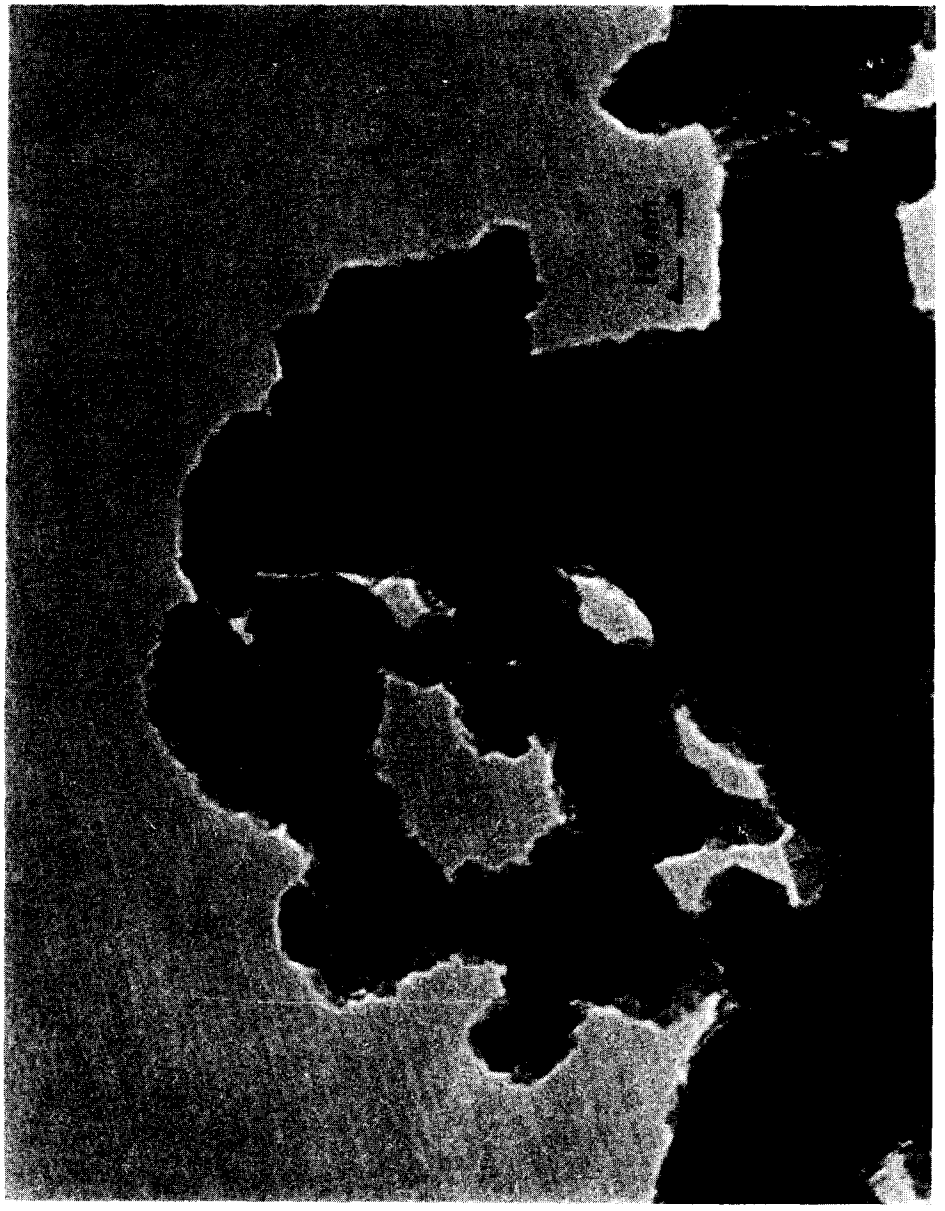

FIG. 15. Photomicrograph of the 1% Rh sample used in Fig. 2 (original magnification $2 \times 10^6$).

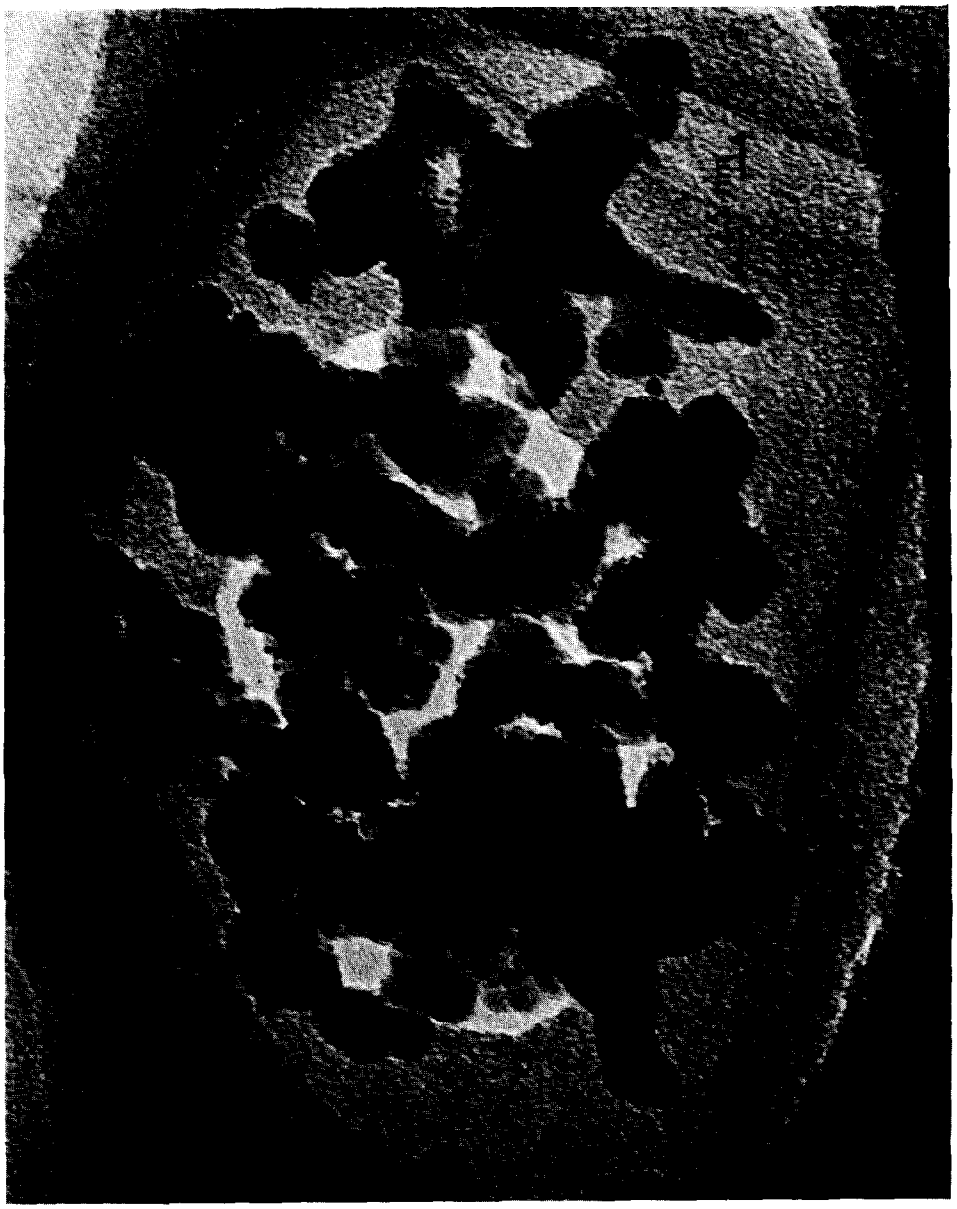

FIG. 16. Photomicrograph of the 10% Rh sample used in Fig. 6 (original magnification $1 \times 10^6$).

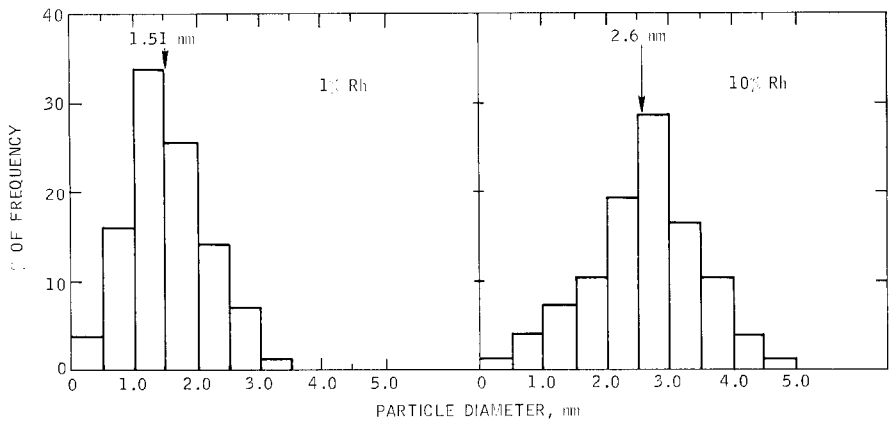


FIG. 17. Particle size distribution for samples of 1% Rh reduced at 200°C (Figs. 2 and 3) and for 10% Rh reduced at 480°C (Figs. 6 and 7) determined by electron microscopy.

we added $N_2$ at pressures up to about 20 cm. If no spectra of adsorbed $N_2$ could be detected, the gaseous $N_2$ was then removed and CO was adsorbed.

Tables 2 and 3 contain the data obtained from the chemisorption of $H_2$ and CO. The data are given as H/M and CO/M. The main feature of this data is the existence of multiple CO adsorption on those samples showing predominantly the 2100 and 2030 $cm^{-1}$ CO bands and its relative absence in samples showing predominantly the 2070 $cm^{-1}$ CO bands.

Figure 17 shows the particle size distribution obtained by electron microscopy of the samples discharged from the infrared cell after CO spectra had been determined. The 1% Rh sample was that used in Figs. 2 and 3, while the 10% Rh sample was that used in Figs. 6 and 7. To allow a direct visual estimate to be made of the contrast achieved, representative micrographs are shown in Figs. 14, 15, and 16.

## DISCUSSION

A classic study by Yang and Garland (*23*) some 20 years ago showed the existence of very complex infrared spectra of carbon monoxide adsorbed on rhodium. In general, except for minor frequency shifts, our spectra are in very close agreement with theirs.

However, we did not study this system because we thought that there were significant deficiencies in their work, but because we thought useful information could be gained by investigating in a more detailed fashion the highly dispersed system exemplified by low concentrations of rhodium on alumina. In addition, we hoped that we would derive synergistic information from a methodology combining infrared studies with chemisorption and microscopy.

As an example, Yang and Garland, entirely on the basis of analogies with the spectrum of rhodium carbonyl chloride, suggested that the two band spectra (in the linear stretching vibration region) of carbon monoxide adsorbed on one of their samples had its origin in the symmetrical and antisymmetrical modes of vibration of two CO molecules bonded to a single rhodium atom. If their assignment is correct, it should be capable of ready verification by chemisorption measurements, provided that the samples used in the two techniques are from the identical starting materials and reduced by identical procedures.

Furthermore, if the concept of multiple CO molecules adsorbed on one rhodium

atom can be verified beyond doubt, it seems to us that this is an extremely interesting phenomena, as, except for ruthenium (*24–26*), there seems to be no transition metal which will definitely adsorb more than one CO molecule on a surface atom. A recent note (*27*) reports the first observations of multiple CO adsorption on iridium.

*Infrared Data*

Our initial experiments were conducted at low temperatures of reduction (200°C) and with a range of rhodium concentrations. In the earlier work of Yang and Garland, they had presented spectra only of 2% Rh reduced at 200°C and of 8% Rh reduced at 400°C. It is unclear to us whether or not the effects they observed in going from 2% Rh to 8% Rh were due to a concentration effect, a temperature effect, or to some combination of these effects.

Figure 1 shows that after reduction of a 10% Rh sample at 200°C, very intense bands of CO were obtained and that the low frequency band varied from 2030 to 2050 $cm^{-1}$, while the high frequency band was coverage invariant at 2100 $cm^{-1}$. A sample containing 1% Rh reduced at 200°C gave greatly simplified spectra when CO was added (Fig. 2). Two bands dominate the spectrum, and they are frequency invariant with coverage. At higher coverages there is a very weak band present at about 2075 $cm^{-1}$. The latter band disappears entirely after a short evacuation at 100°C (Fig. 3) showing that those CO molecules with a stretching frequency of 2100 and 2030 $cm^{-1}$ are more strongly bound to Rh than those CO molecules having a stretching frequency close to 2075 $cm^{-1}$.

While keeping the Rh concentration at 1%, we now inserted a new sample in the cell and reduced it at 480°C for 1 hr. Figure 4 shows that the two frequency invariant bands at 2100 and 2030 $cm^{-1}$ still dominate the spectrum, but that the band at about 2075 $cm^{-1}$ is now present as a clearly resolved, although still overlapped, band. This higher temperature of reduction had no effect on the relative strengths of binding of the various CO species, as the desorption characteristics shown in Fig. 5 are essentially the same as those shown in Fig. 3.

Figure 6 shows the spectra of CO adsorbed on a sample of 10% Rh after reduction at 480°C. Now a band whose frequency varies from 2055 $cm^{-1}$ at low coverage to 2075 $cm^{-1}$ at high coverage dominates the spectrum. The band at 2105 $cm^{-1}$ is clearly present, while the band at 2030 $cm^{-1}$ is resolved only at higher coverage. Desorption studies confirm this picture (Fig. 7), but, at the higher temperatures of evacuation, the 2030 $cm^{-1}$ band is much stronger than the 2100 $cm^{-1}$ band, in marked contrast to the desorption behavior of the dilute Rh samples.

To show that the species of CO giving the band at 2075 $cm^{-1}$ dominate the spectra only when a combination of high concentrations and high temperatures of reduction are used, the following experiment was performed. A sample originally containing 10% Rh was diluted with alumina until the overall Rh concentration was 2%. The sample, after reduction at low temperature (200°C), gave the spectra shown in Fig. 8. In fact, it is of considerable significance that this sample, containing a local concentration of 10% Rh, after reduction at 200°C, shows spectra of adsorbed CO (Fig. 8) almost identical with those obtained with a sample containing 1% Rh reduced at 480°C (Fig. 4). This spectral similarity is also confirmed by the CO chemisorption data shown in Table 2.

Finally, interesting spectroscopic evidence has been found of the effects of adsorbed CO inducing surface mobility of Rh during rereduction. In all samples containing 1% Rh where the initial reduction of the sample was at 200°C, the two band CO spectra were invariably obtained. Figure 11B shows that on rereduction the

system is metastable in that a band at 2055 $cm^{-1}$ associated with less well-dispersed Rh now becomes evident. A second rereduction (Fig. 11C) now produces a spectrum where the 2055 $cm^{-1}$ band is dominant. This striking effect, although as yet not quantitatively entirely understood, shows the sample with adsorbed CO on the Rh goes through a surface reconstruction on rereduction at 200°C. Because of this effect, we did not prepare any samples for spectroscopic studies at high temperatures of reduction from samples that had been initially reduced at 200°C. In summary, we have found a surprising effect of adsorbed CO in enhancing the surface mobility of Rh in hydrogen at 200°C. This has been confirmed by chemisorption studies, as will be discussed later.

The last spectroscopic aspect of these samples that we studied was the adsorption of nitrogen. Apart from a brief note (*16*) concerning $N_2$ adsorbed on silica-supported Rh, no detailed work has been reported on this system. This is somewhat surprising as Rh is one of the metals which is readily obtained in a highly dispersed form. Most studies of adsorbed $N_2$ on metals such as Ni, Ir, and Pt have shown relatively weak bands for $N_2$ adsorbed at room temperature (*17–22*).

Figure 12 shows that a strong band of adsorbed $N_2$ can be obtained readily for 10% Rh on alumina reduced at 500°C. The band is at 2220 $cm^{-1}$. It is of interest that this sample, after evacuation of the $N_2$ and adsorption of CO, showed no band at 2100 $cm^{-1}$. All of the samples we studied which had predominately 2100 and 2030 $cm^{-1}$ bands did *not* adsorb $N_2$. If they did, the adsorbed $N_2$ did not have any bands close to 2200 $cm^{-1}$. Therefore, this shows that only the larger Rh particles can adsorb $N_2$. There seems to be an effect of the support on the infrared spectrum of $N_2$ adsorbed on rhodium, as we have found that in the case of a silica support the stretching band of the $N_2$ is at 2210 $cm^{-1}$. The latter sample contained 10% Rh supported on Cabosil and was reduced at 500°C, following our earlier procedure (*9*). After evacuating the adsorbed nitrogen, CO was added. No band was found at 2100 $cm^{-1}$, indicating a relatively poor dispersion of the rhodium. This we expected from our earlier work (*9*), where a dispersion of about 50% was obtained with no evidence of multiple CO adsorption.

Recently, Smith *et al.* (*28*) have investigated the decarbonylation of $Rh_6(CO)_{16}$ on alumina. They did not refer to Yang and Garland's original infrared studies of supported rhodium (*23*). If they had, it would doubtless have stimulated an interesting comparison with their own studies. Particularly striking is their observation of "one stable intermediate" formed during decarbonylation. Two symmetrical bands of equal intensity were reported for this intermediate at 2080 and 2000 $cm^{-1}$, in close resemblance to the spectra of CO adsorbed on the 2% Rh sample reported by Yang and Garland. This intermediate may well be the raft structure proposed in this paper with the stoichiometry $Rh(CO)_2$. We are trying to establish the CO to Rh stoichiometry for the stable intermediate reported by Watters and co-workers. Initial studies suggest that rhodium carbonyl species migrate during the reduction process (200°C maximum) to give 2.0-nm rhodium particles, based on $H_2$ chemisorption studies. The infrared spectra (*28*) of the decarbonylated rhodium carbonyl chloride dimer supported on Vycor glass, after introduction of CO, are also quite similar to those of CO on highly dispersed Rh reported in this paper. A recent review (*29*) on transition metal cluster complexes also failed to note the striking analogy between the decomposition products of rhodium carbonyls and the work of Yang and Garland.

*Chemisorption Data*

In contrast to such metals as platinum and nickel, very few studies have been

reported on the dispersion and chemisorption stoichiometry of rhodium, either supported or unsupported. Following the original work of Yates and Sinfelt (*9*), who studied both the unsupported Rh and silica-supported Rh, the most detailed work is that of Wanke and Dougharty (*30*), who used alumina as the support. Recently, more work using alumina has been reported by Yao *et al.* (*31*). However, in the latter paper all the samples were precalcined in air before reduction. The inclusion of this calcination step makes comparisons with the earlier work (*9*, *30*) and with the present work difficult.

With unsupported rhodium excellent agreement was found between areas determined by the physical adsorption of argon and the chemisorption of hydrogen (*9*). The assumption used in calculating the areas from the hydrogen chemisorption was the usual one, namely, that the hydrogen dissociated and that one surface Rh atom adsorbs one H atom. As no infrared experiments could be done with unsupported Rh, no attempt was made to use the CO chemisorption data as a method of measuring the particle size.

For the silica-supported samples studied earlier (*9*), the infrared spectra of adsorbed carbon monoxide showed that the linear form of adsorbed CO predominated. Using this fact, we expressed our chemisorption data as the ratio of carbon monoxide molecules per rhodium atom in the catalyst (CO/M) and the corresponding value assuming one atom of hydrogen per metal atom (H/M). Table 1 of Ref. (*9*) shows that for all catalysts except the one containing 0.1% Rh, the CO/M value was either equal to, or a little less than, the H/M values. In these circumstances, there is no evidence of multiple CO adsorption on one Rh atom. On the contrary, mainly linear CO is present, with a significant number of bridged $[(Rh)_2CO]$ species. In this case, each CO molecule is adsorbed on two surface Rh atoms. The only exception to this (*9*) was the sample containing 0.1% Rh, where the H/M ratio was found to be close to unity while the CO/M ratio was 1.4.

As an independent check on the validity of the use of hydrogen chemisorption for determining dispersion (and particle size), some catalysts of relatively poor Rh dispersion were studied (*9*) by X-ray diffraction line broadening. For a 5% Rh catalyst a size of 121 Å was obtained by diffraction, in excellent agreement with the value of 127 Å derived from the hydrogen chemisorption data. It was concluded for both unsupported Rh and silica-supported Rh that the assumption of one H atom to one Rh surface atom was correct (*9*).

However, the work of Wanke and Dougharty (*30*) showed that the situation with alumina-supported rhodium was much more complex. In particular, at Rh concentrations below 1%, the H/M ratio was significantly above 1 for 0.5, 0.1, and 0.02% Rh. No ready explanation was offered (*30*) for these unexpected H/M ratios for low Rh concentration catalysts. However, as there are experimental problems in the use of very low Rh content samples in the infrared, we have studied in this work only samples containing more than 1% Rh. For this reason comparisons with previous data will be confined to the 1–10% Rh concentration range.

Table 2 shows our data for H/M and CO/M where the samples were reduced under conditions identical to those used in the infrared experiments. Because of the effects of surface mobility on rereduction (Fig. 11), a more detailed study than usual was done on chemisorption. For the first group of data shown in Table 2 the procedure was as follows. The initial reduction of a given sample of the 1% Rh sample was done at 200°C, the sample was evacuated at 180°C, and then a hydrogen isotherm was run after cooling to room temperature. The sample was kept in the cell and then rereduced by flowing hydrogen over it at room temperature, then heating to 180°C

using the rate of rise of temperature and hydrogen flow given in the experimental section. Then a CO isotherm was measured at room temperature. This was done five times for five separate samples taken from a master batch of the 1% Rh catalyst. The values in parentheses after the H/M and CO/M values refer to the number of separate samples measured; the numerical value given is the average. Good experimental accuracy was achieved. For example, the five individual values giving the average H/M value of 1.16 are: 1.18, 1.14, 1.15, 1.10, and 1.23. For two of these samples the effect of rereduction after a CO isotherm was studied by performing a second rereduction. The CO/M was then found to be 1.19, a marked drop from the average value of 1.73 for the five samples studied after only one rereduction. Reproducible data were also obtained with the CO isotherms, the individual values of 1.8, 1.65, 1.69, 1.75, and 1.77 giving the average of 1.73.

Reduction of a 1% Rh sample at 200°C leads to the following conclusions: as the H/M value is essentially unity, this means that all the Rh atoms in the sample are in the surface. The simplest way in which this can take place is by postulating an array of Rh clusters all one atom thick. Such two-dimensional rafts have been directly resolved in the electron microscope using a 1% Rh on silica sample (*8*). Evidently, the average number of atoms in each raft must be relatively small, as high CO/M values were measured (1.73). It is unlikely, on elementary steric grounds, that the Rh atoms in the middle of large rafts (say $20 \times 20$ atoms) can adsorb more than one CO molecule per Rh atom. This interpretation is also in good agreement with the spectra of the CO adsorbed on a 1% Rh sample reduced at 200°C.

For a series of 1% Rh samples reduced at 465°C (Table 2), it is interesting that atomic dispersion is still retained under these more severe conditions, as shown by the H/M ratio of 1.0 still being present. However, the CO/M is now found to be 1.46, which is most readily interpreted as an increase in the average number of Rh atoms in the two-dimensional rafts. Again, the infrared data are in good agreement with this interpretation.

For the 10% Rh samples reduced at 200°C, however, atomic dispersion is now absent, the H/M ratio being 0.51. It is possible that this might mean that all of the Rh atoms are in three-dimensional spherical (or cubic) particles of 2.1 nm. This is, however, not so as we measure a CO/M ratio of 0.78, considerably greater than the H/M ratio. Infrared spectra also lead to this conclusion as the bands characteristic of multiple CO adsorption are still strong with this sample. These two experimental techniques therefore indicate that two types of Rh particles must coexist in this sample. One is the two-dimensional rafts and the other is small three-dimensional particles. The relative numbers of Rh atoms in these two types of particles is, of course, not known. In principle, however, it can be determined by electron microscopy, as discussed later. When a sample containing 10% Rh was reduced at 480°C, the overall dispersion of the system as shown by the H/M value of 0.54 is the same as found after the low temperature reduction. This is somewhat surprising and probably indicates that the critical steps which determine the overall dispersion of these samples are those that occur before a reduction temperature of 200°C is reached. However, in dramatic contrast with the 200°C reduction of the same sample, the CO/M ratio is now found to be less than the H/M, 0.46 and 0.54, respectively. This indicates that if multiple CO adsorption is still occurring to a small extent, then the dominating form of chemisorption is probably linear with some bridged CO also present. This will be discussed in more detail in the conclusions. As observed with the 1% Rh samples, both

of the 10% samples showed rearrangement on rereduction after a CO isotherm, as shown by the second CO isotherm. In both cases, these CO/M values were considerably lower than those found after the first CO isotherms.

A summary of our basic chemisorption data together with the relevant literature data is shown in Table 3. After reduction at 500°C, the H/M and CO/M values are not very different for 10% Rh on silica or on alumina (A vs C). For the same reduction temperature the 5% Rh sample on alumina (B) shows considerably higher dispersion than does the silica-supported sample (A). However, no multiple CO adsorption is evident with the alumina samples (B) and (C), but is evident in sample (D) after a low temperature reduction. Much larger differences in samples reduced at 500°C are evident at the 1% Rh loading level. For the silica support (A), the CO/M ratio is only a little larger than the H/M ratio, while for both alumina samples, for two different aluminas (B and C) the CO/M ratio is about 40% more than the H/M ratio. Such values clearly indicate that a considerable amount of multiple CO adsorption is present in the alumina supported Rh, while only small amounts are present on the silica-supported Rh.

Changing the reduction temperature from 470 to 200°C shows dramatic changes in the multiply held CO, while leaving the overall dispersion of the Rh the same. The latter judgment is based on the essential invariance of the H/M values in columns C and D of Table 3. For the 10% samples, a CO/M value of 0.46 was found after 470°C reduction, increasing to 0.78 for samples reduced at 200°C. Corresponding values for the 1% Rh samples are 1.46 and 1.73. Based on the definitions given in the introduction, all of the 1% Rh samples on alumina listed in Table 2 show ultradispersion and are, of course, atomically dispersed in the conventional sense. It is particularly encouraging in assessing the potential universality of this data to note that the 1% Rh samples used by workers in two different laboratories were made on entirely different aluminas using different preparative procedures. Based on the above definition of ultradispersion, it is evident that the main effect of low temperature of reduction at the 1% Rh level is to increase markedly the extent of ultradispersion, as shown by the CO/M value of 1.73 versus the value of 1.46 after the more severe reduction.

## CONCLUSIONS

### *Ultradispersion, Surface Topology, and Electron Microscopy*

The above considerations involving spectroscopy and chemisorption will now be brought into synergistic perspective using one assumption. This is that for two-dimensional rafts of Rh atoms, only edge or corner atoms can and do adsorb two CO molecules. All other Rh atoms in these rafts (the so-called interior atoms) can adsorb only one CO molecule. This argument is essentially steric in origin; there is just not enough space for multiple CO adsorption to occur in the middle of two-dimensional rafts.

From this assumption we can readily construct the simple atomic model of raft structure shown in Fig. 13. This applies to Rh on any support, but is based on the data of Prestridge and Yates (*8*) who measured a Rh–Rh spacing of 0.375 nm for two-dimensional Rh rafts on silica. It is very unlikely that the Rh–Rh distance for Rh rafts on alumina is significantly different from that of Rh rafts on silica. From this model we can also calculate, in an obvious fashion, the CO/M ratio for a given raft and measure its effective diameter from a scale diagram. Evidently such a model should lead to the same conclusions from electron microscopy as from the chemisorption values of CO/M, if our conception of the system is correct.

Detailed electron microscope studies have been performed on the identical samples used in the infrared work and the particle size distributions are shown in Fig. 17. The 1% Rh sample was that used to obtain the spectra shown in Fig. 2 and was reduced at 200°C. The 10% Rh sample was that used in Fig. 6 and was reduced at 480°C. The photomicrographs of the 1% sample (Fig. 15) showed only two-dimensional rafts, no electron-opaque three-dimensional particles being detected. A detailed discussion of the electron microscopy of two-dimensional rafts versus three-dimensional particles is given elsewhere (*32*). This is, of course, in agreement with the hydrogen chemisorption data given in Table 2, where five separate reduction sequences showed that such samples were always atomically dispersed (by hydrogen chemisorption). The number average particle sizes of the rafts is 1.51 nm (see Fig. 17) and particles were found in size ranges varying from 0.7 to 3.5 nm. For the 10% sample (Fig. 16) it is of interest that large numbers of two-dimensional rafts were still seen in the particle size range from 0.7 to 4.0 nm. Particles larger than this were all found to be more than one atom thick, i.e., they are normal three-dimensional entities that one considers as particles. In the size range between 2.0 and 4.0 nm, both rafts and three-dimensional particles were observed. Considerations of the model show that arrays of 4.0 nm in size contain 81 atoms, i.e., if square they would form a 9 × 9 atom raft. However, examination of the electron micrographs shows that the most probable shape is round. Above this size, it appears that Rh attains a lower energy configuration by always collecting into three-dimensional entities. Intermediate behavior was found with intermediate raft sizes where a given particle size can result from either three-dimensional or two-dimensional entities.

Figure 18 shows how the CO/M ratio varies with the number of Rh atoms in a raft, based on the assumption that only rafts exist. This is essentially correct for the 1% Rh samples studied in this work for both temperatures of reduction. Rafts containing from 1 to 7 atoms have a CO/M of 2, 8 and 9 of 1.9, 10 and 12 of 1.8, with a slow decrease above this. For example, using this model one finds a CO/M of about 1.7 for a 20-atom raft, 1.6 for a 29-atom raft, falling to 1.5 for a 46-atom raft. With Rh on $Al_2O_3$ it proved to be more difficult than with Rh on $SiO_2$ to resolve individual atoms (*8*), so in this work we measured the diameter of the rafts, rather than count atoms directly. Hence, we constructed the plot shown in Fig. 19 where CO/M is shown as a function of raft diameter for the two-dimensional Rh system.

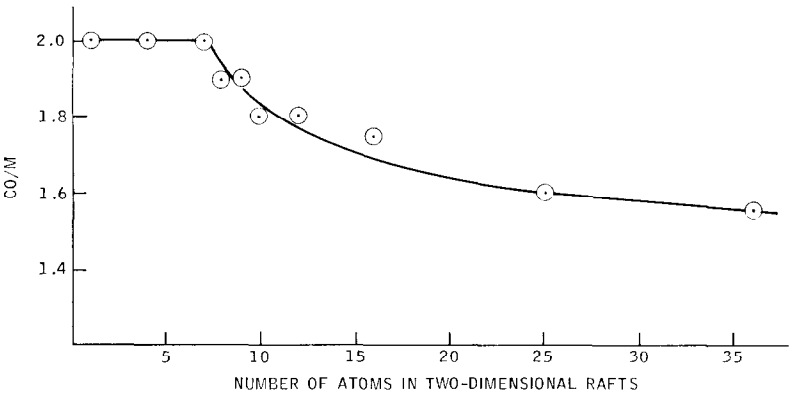


FIG. 18. CO/M ratio versus the number of atoms in rhodium rafts.

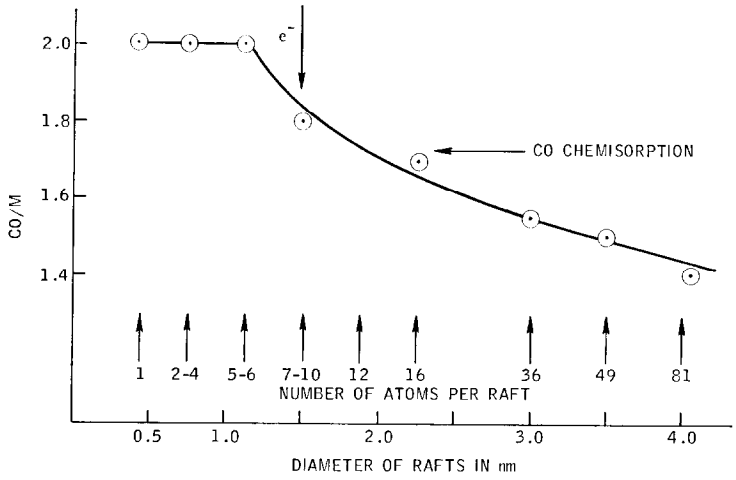


FIG. 19. CO/M ratio for two-dimensional rhodium rafts as a function of their diameter.

The data of Fig. 17 show a number average raft size of 1.51 nm, corresponding to the average size raft containing 7 to 10 atoms. It will be seen from Fig. 13 that all of these rafts have the same size. From the smoothed curve of Fig. 19, this would correspond to a CO/M value of 1.8. In other words the electron microscope data on the sample used for the CO spectra shown in Fig. 2 predict that the sample would have a CO/M ratio of 1.8. Of course this cannot be measured accurately on a sample weighing some 0.015 g. However, the average of five separate chemisorption determinations using larger samples from the same batch of catalyst showed a CO/M ratio of 1.73 (Table 2). We consider that this is a very satisfactory agreement and that this system (1% Rh on $Al_2O_3$ reduced at 200°C) is the best defined example of an ultradispersed metal that we know of.

In summary we have found by a combination of infrared spectroscopy, chemisorption, and electron microscopy that a 1% Rh on alumina catalyst has all of its Rh atoms in rafts one atom thick. The existence of these rafts is strongly suggested by hydrogen chemisorption and directly confirmed by electron microscopy. The infrared spectra of adsorbed CO also make it very probable that the most likely arrangement of the Rh atoms is as rafts. Direct examination by electron microscopy showed that indeed the rafts exist, and that their average size is 1.5 nm. Consideration of a simple close-packed model of the rafts then predicts a CO/M ratio of 1.8, in very good agreement with the measured average value of 1.73.

The attainment of an average raft size of about 1.0 nm would give a system having the ultimate in ultradispersion, namely every Rh atom would be an edge or corner atom as shown by a CO/M value of 2. This, of course, assumes that the stoichiometry of carbon monoxide adsorption on rhodium does not change for these rafts containing six or less Rh atoms.

## REFERENCES

1. Spenadel, L., and Boudart, M., *J. Phys. Chem.* 64, 204 (1960).
2. Adler, S. F., and Keavney, J. J., *J. Phys. Chem.* 64, 208 (1960).
3. Gruber, H. L., *J. Phys. Chem.* 66, 48 (1962).
4. Adams, C. R., Benesi, H. A., Curtis, R. M., and Meissenheimer, R. G., *J. Catal.* 1, 336 (1962).
5. Wilson, G. R., and Hall, W. K., *J. Catal.* 17, 190 (1970).
6. van Hardeveld, R., and Hartog, F., *Surf. Sci.* 15, 189 (1969).
7. Anderson, J. R., "Structure of Metallic Catalysts," p. 244. Academic Press, New York, 1975.

*8.* Prestridge, E. B., and Yates, D. J. C., *Nature (London)* **234**, 345 (1971).
*9.* Yates, D. J. C., and Sinfelt, J. H., *J. Catal.* **8**, 348 (1967).
*10.* Yates, D. J. C., *J. Colloid Interface Sci.* **29**, 195 (1969).
*11.* Yates, D. J. C., Taylor, W. F., and Sinfelt, J. H., *J. Amer. Chem. Soc.* **86**, 2996 (1964).
*12.* Damrel, J. B., *Instruments Controls* **36**, 87 (1963).
*13.* Guerra, C. R., and Schulman, J. H., *Surf. Sci.* **7**, 229 (1967).
*14.* Garland, C. W., Lord, R. C., and Troiano, P. F., *J. Phys. Chem.* **69**, 1188 (1965).
*15.* Harrod, J. F., Roberts, R. W., and Rissman, E. F., *J. Phys. Chem.* **71**, 343 (1967).
*16.* Borod'ko, Yu. G., and Lyutov, V. S., *Kinet. Catal.* **12**, 238 (1971).
*17.* Eischens, R. P., and Jacknow, J., "Proc. 3rd Int. Congress on Catalysis," Vol. 1, p. 627. North Holland, Amsterdam, 1965.
*18.* van Hardeveld, R., and van Montfoort, *Surf. Sci.* **4**, 396 (1966).
*19.* Mertens, F. P., and Eischens, R. P., *in* "The Structure and Chemistry of Solid Surfaces" (G. A. Somorjai, Ed.). Wiley, New York, 1969.
*20.* Eischens, R. P., *Accounts Chem. Res.* **5**, 74 (1972).
*21.* Egerton, T. A., and Sheppard, N., *J. Chem. Soc. Faraday Trans. I.* **7**, 1357 (1974).
*22.* Ravi. A., King, D. A., and Sheppard, N., *Trans. Faraday Soc.* **64**, 3358 (1968).
*23.* Yang, A. C., and Garland, C. W., *J. Phys. Chem.* **61**, 1504 (1957).
*24.* Kobayashi, M., and Shirasaki, T., *J. Catal.* **28**, 289 (1973).
*25.* Kobayashi, M., and Shirasaki, T., *J. Catal.* **32**, 254 (1974).
*26.* Dalla Betta, R. A., *J. Phys. Chem.* **79**, 2519 (1975).
*27.* Anderson, J. R., and Howe, R. F., *Nature (London)* **268**, 129 (1977).
*28.* Smith, G. C., Chojnacki, T. P., Dasgupta, S. R., Iwatate, K., and Watters, K. L., *Inorg. Chem.* **14**, 1419 (1975).
*29.* Smith, A. K., and Basset, J. M., *J. Mol. Catal.* **2**, 229 (1977).
*30.* Wanke, S. E., and Dougharty, N. A., *J. Catal.* **24**, 367 (1972).
*31.* Yao, H. C., Japar, S., and Shelef, M., *J. Catal.* **50**, 407 (1977).
*32.* Prestridge, E. B., Via, G. H., and Sinfelt, J. H., *J. Catal.* **50**, 115 (1977).